Internal dynamics of multibarrier systems for pulsed quantum decay

Gastón García-Calderón,[1,*] Roberto Romo,[2,†] and Jorge Villavicencio[2,‡]
[1]*Instituto de Física, Universidad Nacional Autónoma de México, Apartado Postal 20 364, 01000 México, D.F., Mexico*
[2]*Facultad de Ciencias, Universidad Autónoma de Baja California, Apartado Postal 1880, 22800 Ensenada, Baja California, Mexico*
(Received 21 November 2007; revised manuscript received 29 January 2009; published 26 May 2009)

An exact analytical approach is used to explore the dynamics of the decaying probability density and the probability current in multibarrier systems. We show that resonance state interference produces the appearance of *breathing* or *bouncing* modes in the dynamical behavior of the probability density along the internal region of the system. This dynamical process involves the reconstruction of the initial state and it is responsible for the pulsed features of the decay recently discussed for the *survival probability* in these systems.

DOI: 10.1103/PhysRevA.79.052121 PACS number(s): 03.65.−w, 73.21.Cd, 73.40.Gk

I. INTRODUCTION

The time evolution of quantum decay is a subject as old as quantum mechanics. At the end of the twenties of the last century, the problem of α decay in radioactive atomic nuclei led to a theoretical derivation of the exponential decay law [1,2]. In the 1950s, Khalfin [3] pointed out the approximate validity of the exponential decay law. It was argued that deviations from this law should occur both at very short and at very long times compared with the lifetime of the decaying system. These theoretical predictions have been confirmed experimentally in recent years in both the short [4] and the long time [5] regimes.

Most theoretical treatments of decay consider the time evolution of an initial state by tunneling out of single well [6–9]. However, the present-day possibility of designing the potential parameters of artificial quantum systems [10] opens the way to study the issue of decay in more complex potential profiles as exemplified by semiconductor multibarrier systems of finite length which are formed by a succession of alternating barriers and wells.

A possible way to create an initial state is by laser excitation in one of the quantum wells of the system [11,12]. This occurs essentially in an instantaneous fashion and the subsequent time evolution of the initial state leads in general to a complex dynamics of the probability density along the internal region of the system which is linked the decay process through the edges of the system.

In a recent work [13] we considered an analytical approach to study the time evolution of the survival probability in multibarrier systems along the full time interval, i.e., from $t=0$ to $t=\infty$. We found a decaying regime characterized by a pulsed nonexponential behavior of the survival probability which is caused by transitions among the closely lying resonance levels of the multibarrier system. The survival probability, which yields the probability that at time t the decaying particle remains in its initial state, is a quantity that depends solely on time and hence it provides no information of how the initial decaying state evolves both in position and time within the system to generate that pulsed behavior of decay.

In this work we address the issue of the time evolution of the probability density and the probability current along the internal region of multibarrier systems to elucidate the internal dynamics that originates the pulsed behavior of decay exhibited by the survival probability. We find that the decaying process through the edges of the system is characterized by a dynamical reconstruction of the initial state that exhibits *breathing* or *bouncing* modes for the time evolution of the probability density. We also demonstrate that the evolution of these modes is governed by a complex interference process that depends both on time and the position-dependent phases of the resonance states of the system.

The paper is organized as follows. Section II provides a brief account of the formalism. Sections II A–II C provide, respectively, the relevant expressions for the probability density, the probability current density, and the survival probability. Section III deals with examples and its discussion, and involves subsections on the resonance spectrum and the dynamics of the internal region. Finally, Sec. IV presents the concluding remarks.

II. FORMALISM

We begin this section by presenting, for the sake of completeness, the basic formulas of our approach and establishing the notation to be used in order to derive the analytical expressions for the decaying probability density and the decaying probability current density. These are the relevant quantities that we shall consider to study the internal dynamics of the decaying particle in multibarrier systems.

We consider the decaying solution $\psi(x,t)$ of the time-dependent Schrödinger equation for decay of an initial state $\psi(x,t=0)$, confined along the internal region, $0 \le x \le L$, of a one-dimensional potential $V(x)$ of finite range. The solution $\psi(x,t)$ may be written in terms of $g(x,x';t)$, the retarded Green's function of the problem, as

$$\psi(x,t) = \int_0^L g(x,x';t)\psi(x',0)dx'. \tag{1}$$

The retarded Green's function may be conveniently written as [14]

*gaston@fisica.unam.mx
†romo@uabc.mx
‡villavics@uabc.mx

$$g(x,x';t) = \sum_{n=1}^{\infty} u_n(x)u_n(x')e^{-i\mathcal{E}_n t/\hbar}e^{-\Gamma_n t/2\hbar} + R_n(x,t),$$

$$0 \le [x,x'] \le L, \tag{2}$$

where the functions $u_n(x)$ stand for resonance states, which are defined as solutions to the Schrödinger equation of the problem obeying outgoing boundary conditions at the edge points of the system: $[du_n(x)/dx]_{x=0} = -ik_n u_n(0)$, and $[du_n(x)/dx]_{x=L} = ik_n u_n(L)$. Here k_n represents the complex wave number $k_n = (a_n - ib_n)$ and hence the energy becomes $E_n = \hbar^2 k_n^2/2m = \mathcal{E}_n - i\Gamma_n/2$, where m represents the mass, $\mathcal{E}_n$ the energy, and Γ_n the width, respectively, of the decaying particle. The expansion given by Eq. (2) holds for any points (x,x') along the interval $(0,L)$ except at the points $x = x' = 0 = L$. One should also note that the k_n's correspond also to the complex poles of the outgoing Green's function of the problem and that the residue of this function at the poles, which is proportional to the u_n's, yields the normalization condition for these states [15],

$$\int_0^L u_n^2(x)dx + i\frac{u_n^2(0) + u_n^2(L)}{2k_n} = 1. \tag{3}$$

The term $R_n(x,t)$ in Eq. (2) refers to nonexponential contributions which are only relevant at extremely short and at very long times compared with the lifetime of system [9,14], and hence it can be ignored in the present analysis concerning only the intermediate times decaying regime. Hence, substitution of the discrete sum of Eq. (2) into Eq. (1) leads to a representation involving an infinite number of resonance terms. Hence, along the internal region $(0,L)$ of the system the time-dependent solution $\psi(x,t)$ may be expressed as

$$\psi(x,t) = \sum_{n=1}^{\infty} C_n u_n(x)e^{-i\mathcal{E}_n t/\hbar}e^{-\Gamma_n t/2\hbar} \tag{4}$$

where the expansion coefficients

$$C_n = \int_0^L \psi(x,0)u_n(x)dx, \tag{5}$$

fulfill the relationship [9],

$$\sum_{n=1}^{\infty} \mathrm{Re}\{C_n\bar{C}_n\} = 1, \tag{6}$$

where $\bar{C}_n = \int_0^L \psi^*(x,0)u_n(x)dx$. Clearly, if $\psi(x,0)$ is real then $\bar{C}_n = C_n$.

It is well known that the resonance spectrum of a multibarrier system, say with $M+1$ barriers, exhibits groups or "minibands" involving each M resonance levels. Following Eq. (6), an initial state $\psi(x,0)$ of energy E_0 will overlap strongly with the closely lying resonance levels than with those situated far away. Without loss of generality one may consider the case of an initial state lying close to the lowest energy miniband of a multibarrier and hence the sum rule given by Eq. (6) may be written to an excellent approximation as

$$\sum_{n=1}^{M} \mathrm{Re}\{C_n\bar{C}_n\} \approx 1. \tag{7}$$

If necessary the above sum may be extended to include the resonance levels of nearby minibands.

The above means that it is sufficient to consider a finite number of terms in the expression for the time-dependent solution given by Eq. (4), namely,

$$\psi(x,t) \approx \sum_{n=1}^{M} C_n u_n(x)e^{-i\mathcal{E}_n t/\hbar}e^{-\Gamma_n t/2\hbar}. \tag{8}$$

A. Probability density

The internal dynamics is described by the probability density $|\psi(x,t)|^2$ as a function of both position and time. The corresponding analytical expression follows from Eq. (4) and may be written as

$$|\psi(x,t)|^2 = \rho^{\exp}(x,t) + I^{Rabi}(x,t), \tag{9}$$

where $\rho^{\exp}(x,t)$ stands for the purely exponentially decaying contributions,

$$\rho^{\exp}(x,t) = \sum_{n=1}^{M} |C_n|^2|u_n(x)|^2e^{-\Gamma_n t/\hbar}, \tag{10}$$

and $I^{Rabi}(x,t)$ describes the interference contribution formed by decaying Rabi-type oscillatory contributions,

$$I^{Rabi}(x,t) = 2\sum_{n,m>n}^{M} |C_m^* C_n u_m^*(x)u_n(x)|e^{-\bar{\Gamma}_{mn}t/\hbar}\cos[\Phi_{mn}(x,t)], \tag{11}$$

with

$$\Phi_{mn}(x,t) = \Omega_{mn}t + \beta_{mn}(x) + \alpha_{mn}, \tag{12}$$

where the different phases above are defined through the expressions $u_m^*(x)u_n(x) = |u_m^*(x)u_n(x)|\exp[i\beta_{mn}(x)]$ and $C_m^*C_n = |C_m^*C_n|\exp(i\alpha_{mn})$, and Ω_{mn} stands for the *Rabi frequency* defined as

$$\Omega_{mn} = (\mathcal{E}_m - \mathcal{E}_n)/\hbar. \tag{13}$$

Also, in Eq. (11), $\bar{\Gamma}_{mn}$ is the mean of the widths of the corresponding interacting resonances,

$$\bar{\Gamma}_{mn} \equiv (\Gamma_m + \Gamma_n)/2. \tag{14}$$

B. Probability current density

Integrating the probability density $|\psi(x,t)|^2$ along the internal region of the system yields the *nonescape probability*

$$P(t) = \int_0^L |\psi(x,t)|^2 dx. \tag{15}$$

This quantity provides the probability that at time t the particle is inside the system.

The time dependence of $dP(t)/dt$ provides information about the actual flux through the edges of the system, since it is connected with the probability current density $J(x,t)$, by the well known expression

$$\frac{d}{dt}P(t) = J(0,t) - J(L,t), \tag{16}$$

where

$$J(x,t) = (\hbar/m)\mathrm{Im}[\psi^*(x,t)(\partial/\partial x)\psi(x,t)]. \tag{17}$$

This is an interesting quantity because it allows to determine whether the decayed flux, either at $x=0$ or $x=L$, is able to return inside the system. Substituting Eq. (4) into Eq. (17) allows to write the probability current density, say at $x=L$, as

$$J(L,t) = J^{\exp}(L,t) + J^{Rabi}(L,t), \tag{18}$$

where $J^{\exp}(L,t)$ consists of a purely decaying contribution,

$$J^{\exp}(L,t) = \frac{\hbar}{m}\sum_{n}^{M} |C_n|^2 |u_n(L)|^2 a_n e^{-\Gamma_n t/\hbar}, \tag{19}$$

and $J^{Rabi}(L,t)$ refers to the interference term that involves the decaying Rabi contributions,

$$J^{Rabi}(L,t) = \frac{\hbar}{m}\sum_{m\neq n,n}^{M} |B_{mn}|\cos(\Omega_{mn}t + \eta_{mn})e^{-\bar{\Gamma}_{mn}t/\hbar}, \tag{20}$$

where $B_{mn}=|B_{mm}|\exp(i\eta_{mn})$ with $|B_{mn}| \equiv |C_m u_m(L) C_n u_n(L) k_n|$, and η_{mn} the corresponding phase. A similar procedure follows for $x=0$. For symmetric multibarrier systems with the initial state seated on the central well, as considered in an example of next section, the value of the outward flux is the same at $x=0$ and $x=L$ but with opposite sign, namely, $J(0,t)=-J(L,t)$, so that it is sufficient to analyze the flux in one of these points, say $x=L$.

C. Survival probability

In order to complete the analysis of the internal dynamics of the decaying particle it is convenient to refer also to the survival probability defined by

$$S(t) = \left| \int_0^L \psi^*(x,0)\psi(x,t)dx \right|^2. \tag{21}$$

This quantity provides the probability of finding the decaying particle in its initial state at time t. Substitution of Eq. (4) into Eq. (21) yields the expression

$$S(t) = \sum_{n=1}^{M} |C_n \bar{C}_n|^2 e^{-\Gamma_n t/\hbar} + 2\sum_{m>n,n}^{M} |D_{mn}| e^{-\bar{\Gamma}_{mn}t/\hbar} \times \cos(\Omega_{mn}t + \xi_{mn}), \tag{22}$$

where $D_{mn}=|D_{mn}|\exp(i\xi_{mn})$, $|D_{mn}|=|C_m\bar{C}_m C_n\bar{C}_n|$ and ξ_{mn} corresponds to the phase difference between that of $C_m\bar{C}_m$ and $C_n\bar{C}_n$.

It is worth noticing the differences in the phase dependence of the analytical expressions for probability density, the current probability density, and the survival probability given, respectively, by Eqs. (11), (20), and (22).

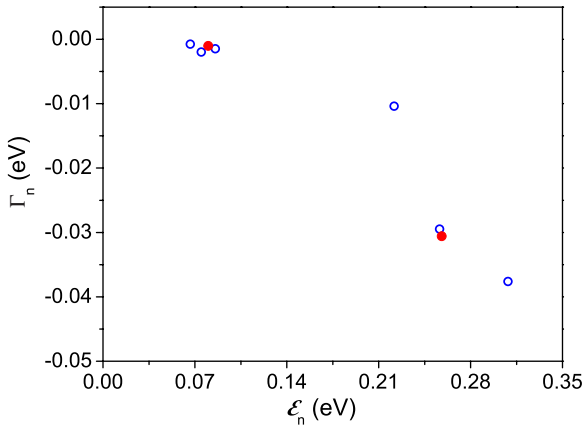

FIG. 1. (Color online) Complex energy poles $\mathcal{E}_n, \Gamma_n$ for the first two triplets of a quadruple-barrier system (circles) and the first two poles of a double-barrier resonant system (dots).

III. EXAMPLE AND DISCUSSION

In order to exhibit the dynamical behavior of the probability density along the internal region of a multibarrier system, we find convenient, without loss of generality, to refer to a specific multibarrier system. We consider a symmetrical quadruple-barrier resonant tunneling system (QBRTS), namely, a system formed by four barriers alternating with three wells, characterized by parameters typical of semiconductor heterostructures [10]: barrier heights $V_0=200$ meV, barrier widths $b_0=4.0$ nm, and well widths $w_0=5.0$ nm. The effective mass is $m^*=0.067m_e$, with m_e as the electron mass.

A. Resonance spectrum

It is important to stress out that for the above behavior to be accomplished, the structure of the resonance spectrum is of critical importance. It explains for example why systems with two or more quantum wells are quite capable of exhibiting Rabi oscillations, while for systems consisting on a single well this phenomenon is hard to occur. Since in our example there are three wells, the energy spectra group in sets of three resonance levels. Figure 1 exhibits the resonance parameters $(\mathcal{E}_n, \Gamma_n)$ on the complex energy plane corresponding to the first two triplets. Note that the first resonance triplet lies below the potential height and for that reason its widths are much smaller than those of the second triplet. The resonance parameters of the first energy triplet, which exhibits relatively sharp and isolated resonances, are $\mathcal{E}_1=66.49$ meV and $\Gamma_1=0.737$ meV; $\mathcal{E}_2=74.87$ meV and $\Gamma_2=1.96$ meV; $\mathcal{E}_3=85.54$ meV and $\Gamma_3=1.45$ meV; and those of the second triplet, which are much broader and overlap with each other: $\mathcal{E}_4=221.69$ meV and $\Gamma_4=10.38$ meV; $\mathcal{E}_5=256.44$ meV and $\Gamma_5=29.48$ meV; $\mathcal{E}_6=308.3$ meV and $\Gamma_6=37.62$ meV. Notice that Γ_1 is the smallest resonance width and hence it yields the longest lifetime of the system, $\tau_1 \equiv \hbar/\Gamma_1 = 1.1197$ ps.

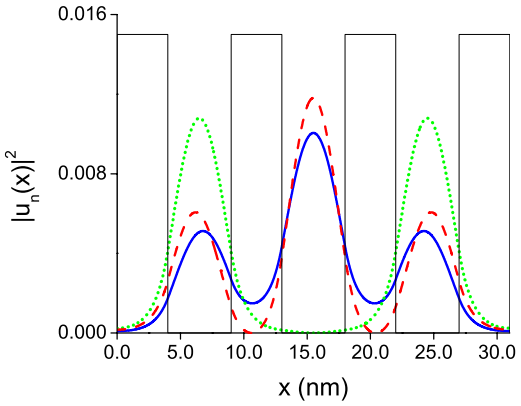

FIG. 2. (Color online) The resonance states $|u_n(x)|^2$ of the quadruple-barrier system, with parameters specified in the text, are plotted along the internal region: $n=1$ (solid line), $n=2$ (short-dotted), and $n=3$ (dashed). The potential profile is also shown to help the eye (solid line).

Figure 1 also shows, for comparison, the first two complex energy poles of a double-barrier resonant system with barrier heights $V_0=0.23$ eV, and barrier and well widths, $b=w=5.0$ nm. The corresponding resonance parameters are $\mathcal{E}_1=80.05$ meV and $\Gamma_1=1.028$ meV; $\mathcal{E}_2=258.0$ meV and $\Gamma_2=30.58$ meV. This is a typical case of poles for systems having a single well and explains why these systems [16] do not exhibit Rabi oscillations. Usually the initial state $\psi(x,0)$ overlaps strongly with the lowest resonance state $u_1(x)$, which means from Eq. (6) that Re $C_1\bar{C}_1\approx 1$, and since $\Gamma_1 \ll \Gamma_2 \ll \Gamma_3\ldots$, it follows from Eq. (10) that the exponential decay contribution is dominated by the term $n=1$. It follows then that the Rabi contribution given by Eq. (11) is negligible since $\bar{\Gamma}_{12}$, defined by Eq. (14), is dominated by Γ_2, which gives a contribution that decays much faster than that regarding Γ_1, and similarly for the rest of resonance contributions.

For the quadruple barrier system the situation is different because there the initial state overlaps mainly with the resonance states of the first triplet and since the widths of these states are comparable with each other, the Rabi contribution is as relevant as the purely decaying exponential contributions. Eventually, however, at longer times the pole with the shortest resonance width dominates the decay.

In addition to the complex energy poles $\{E_n\}$, the resonance states $\{u_n(x)\}$ constitute the other ingredient necessary to calculate the time evolution of $|\psi(x,t)|^2$, $J(x,t)$, and $S(t)$ mentioned in the previous section. Figure 2 exhibits a plot of the resonance states $|u_n(x)|^2$ of the first triplet of resonances along the internal region of the quadruple barrier resonant system: $n=1$ (solid line), $n=2$ (dashed line), and $n=3$ (dotted line). Actually, these states are coupled with the external regions through the boundary conditions given below Eq. (2), though the scale utilized conceals that.

B. Dynamics of the internal region

As mentioned in the introduction, the initial decaying state $\psi(x,0)$ may be formed by ultrashort pulse excitation

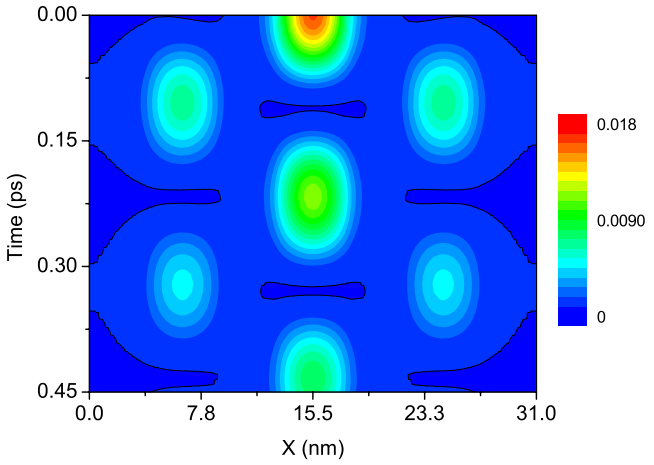

FIG. 3. (Color online) *Breathing* mode of the probability density $|\psi(x,t)|^2$, along the internal region of a QBRTS when the initial state is placed on the central well. One observes that the internal dynamics consists of quasiperiodical processes involving spatial oscillations leading to the reconstruction of the initial state. Note the leakage through the ends of the system in each oscillation.

[11]. A convenient simple model for the initial state $\psi(x,0)$ is the square box ground state,

$$\psi(x,0)=\left(\frac{2}{w_0}\right)^{1/2}\sin[k_0(x-x_0)+\pi/2], \tag{23}$$

for $|x-x_0|<w_0/2$ and zero elsewhere, and x_0 refers to the center of a well of width w_0. An advantage of this initial state is that it leads to simple analytical expressions for the expansion coefficients given by Eq. (5). Using a somewhat more realistic initial state, such as a Gaussian wave packet, will not modify the above considerations provided it is essentially confined within the well.

1. Breathing mode

For the particular choice $x_0=2b_0+3w_0/2$ and $k_0=\pi/w_0$, the initial pulse $\psi(x,0)$ becomes the ground state of a quantum box that fits exactly in the central well of the system. It is then straightforward to show that the coefficients C_n are proportional to $u_n(x_0)$ implying that when the pulse is placed at the center of a symmetrical potential, all C_n with n even will vanish. This is a consequence of the fact that x_0 becomes a node of all the antisymmetrical u_n's and hence it originates a *selection rule* which dictates that only transitions between resonant states with n odd will be allowed in this case.

Figure 3 exhibits the time-dependent probability density plotted as a function of both position and time for the first few oscillations calculated using Eqs. (9), (10), and (13). The regular oscillations exhibited by the probability density $|\psi(x,t)|^2$ have a well defined frequency, which coincides with the Rabi period $T_{13}=0.217$ ps associated to transitions between the states $n=1$ and $n=3$. Note that Rabi oscillations involving the state $n=2$ are forbidden by the selection rule mentioned above, and hence C_2^2 vanishes in this case. On the other hand, Re$(C_1^2)=0.3537$ and Re$(C_3^2)=0.3994$, so the sum rule given by Eq. (6) is ≈ 0.75, which means that these states take most of the strength.

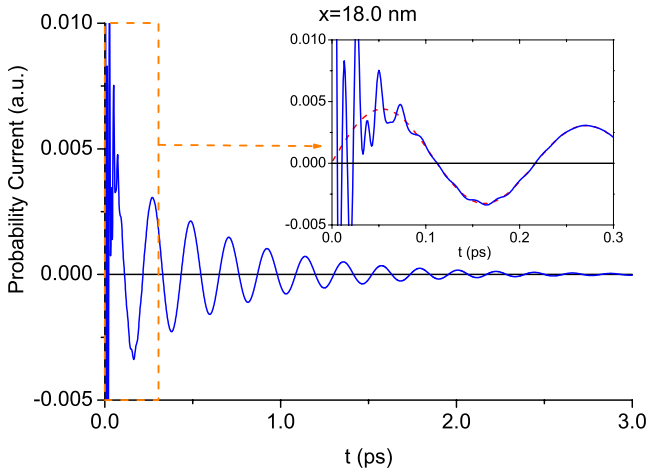

FIG. 4. (Color online) Probability current at the right edge of the central well, $x_c=18.0$ nm. Here we have a bidirectional flux that accounts for the buildup process of the periodic reconstruction of the initial state, a process that occurs at the Rabi frequency Ω_{13}. The inset shows Rabi oscillations of higher frequencies due to transitions among far away resonances. Here we compare the calculation with $N=3$ (dashed red line) and $N=9$ (solid blue line).

The Rabi oscillations exhibited in Fig. 3 are the manifestation of a quasiperiodic reconstruction of the initial state. It is worth noticing that the contour line that goes to the edges of the system illustrating the leakage of the probability density via tunneling each time the probability density "hits" the lateral barriers. Two stages are clearly identified in each Rabi period: (i) at half a cycle ($t=T_{13}/2\simeq 0.108$ ps) the initial pulse is split symmetrically into two smaller "replicas" in the flanking wells, where part of the probability density escapes out of the system via tunneling through the external barriers, and (ii) the rest comes back to the central well leading to a partial reconstruction of the initial state, so that the probability density builds up again in the central well when the cycle is completed ($t=T_{13}\simeq 0.22$ ps). This cyclic process repeats periodically with time while the amplitude of the subsequent maxima of $|\psi(x,t)|^2$ decreases exponentially.

If an integration of the continuity equation is performed in a small region involving only the central well, that is from $x_l=2b_0+w_0$ to $x_r=2b_0+2w_0$, then the probability current density say at $x=x_r$, $J(x_r,t)$, provides precise information on the reconstruction of the initial state and similarly for $x=x_l$. A graph of $J(x_r,t)$ vs t is depicted in Fig. 4 in order to illustrate the internal dynamics discussed above. In this case, the oscillatory behavior is also dominated by the Rabi frequency Ω_{13}. As the inset shows, other Rabi frequencies manifest themselves at shorter time intervals. In this case, small oscillations with frequency Ω_{35} appear at times below 0.2 ps and evidence of Ω_{37} also begins to be visible at times around 0.05 ps, an effect that is small in the relevant time interval. The dominance of a particular Rabi frequency over the rest depends on some factors such as the values of the coefficients C_n and of the widths Γ_n of the resonance states, which as discussed above, in our example are the states $n=1$ and $n=3$, that explains why they are dominant here.

2. Interference of resonance states

The resonant states $u_n(x)$ play a crucial role on the dynamical behavior in the internal region, especially their mutual interference $u_n(x)u_m^*(x)$, which elucidates the underlying mechanism of the observed oscillations of the spatial and time-dependent probability density $|\psi(x,t)|^2$. Notice how in Fig. 2 the dominant states, $n=1$ and $n=3$, have a strong presence in the central well as is evident for the maximum values of both $|u_1(x)|^2$ and $|u_3(x)|^2$ in that region. However, the time-dependent wave function $\psi(x,t)$, which is formed mainly from a superposition of $u_1(x)$ and $u_3(x)$, namely, from Eq. (4),

$$\psi(x,t)\approx C_1u_1(x)e^{-i\mathcal{E}_1t/\hbar}e^{-\Gamma_1t/2\hbar}+C_3u_3(x)e^{-i\mathcal{E}_3t/\hbar}e^{-\Gamma_3t/2\hbar} \tag{24}$$

yields a probability density $|\psi(x,t)|^2$ that leaves the central well almost completely empty at certain times when it is split symmetrically in the lateral wells. As we see in Fig. 3, this occurs for example at $t=T_{31}/2=0.108$ ps, $t=3T_{31}/2=0.325$ ps, and so on. The above can only be explained as a result of a destructive interference that occurs at these specific times, in which the phases of the involving resonant states play a relevant role. The above implies that the clarification of the connection between the spatial oscillations of $|\psi(x,t)|^2$ inside the system and the dynamics of the decay process needs to consider the combined effect of various quantities involved in the Rabi term of Eq. (11). In this sense, not only the Rabi frequency Ω_{31} is important, but also the position-dependent phase $\beta_{31}(x)$ of the complex product $u_3^*(x)u_1(x)$, as well as the constant phase α_{31} of the product $C_3^*C_1$.

Figure 5(a) shows the displacement of $u_3^*(x)u_1(x)$ in the complex plane as x varies along the whole interval $[0,L]$. As indicated by the arrows, the curve is traced twice in opposite directions: the upper arrow indicates the displacement of this complex product when the parameter x goes from 0 to $L/2$, and the lower arrow indicates the direction when x varies from $L/2$ to L. This back and forth movement of $u_3^*(x)u_1(x)$ between the first and second quadrants originates pronounced variations on the position-dependent phase $\beta_{31}(x)$ when the product crosses the imaginary axis, giving to $\beta_{31}(x)$ a steplike structure depicted in the inset of Fig. 5(a). Figures 5(b) and 5(c) show the effect of this behavior on the oscillatory function responsible for the Rabi oscillations at different times, in particular at $t=0$ when $|\psi(x,t)|^2$ is maximum in the central well, and $t=T_{31}/2$ when the central well is empty. The effect of the modulus of $u_3^*(x)u_1(x)$ on the shape of the oscillating pulses is evident in Fig. 5(d). The strong negative values that this function takes in the central well at $t=T_{31}/2$ is such that $I^{Rabi}(x,t)$, given by Eq. (11), virtually cancels the (positive) exponential contributions $\rho^{\exp}(x,t)$, given by Eq. (10), leaving the probability density $|\psi(x,t)|^2$, given by Eq. (9), almost empty along the central well while at the same time, this function peaks in both lateral wells. This situation repeats periodically, at $t=3T_{31}/2,5T_{31}/2,7T_{31}/2,\ldots$, alternating with a partial reconstruction of the initial state due to decay.

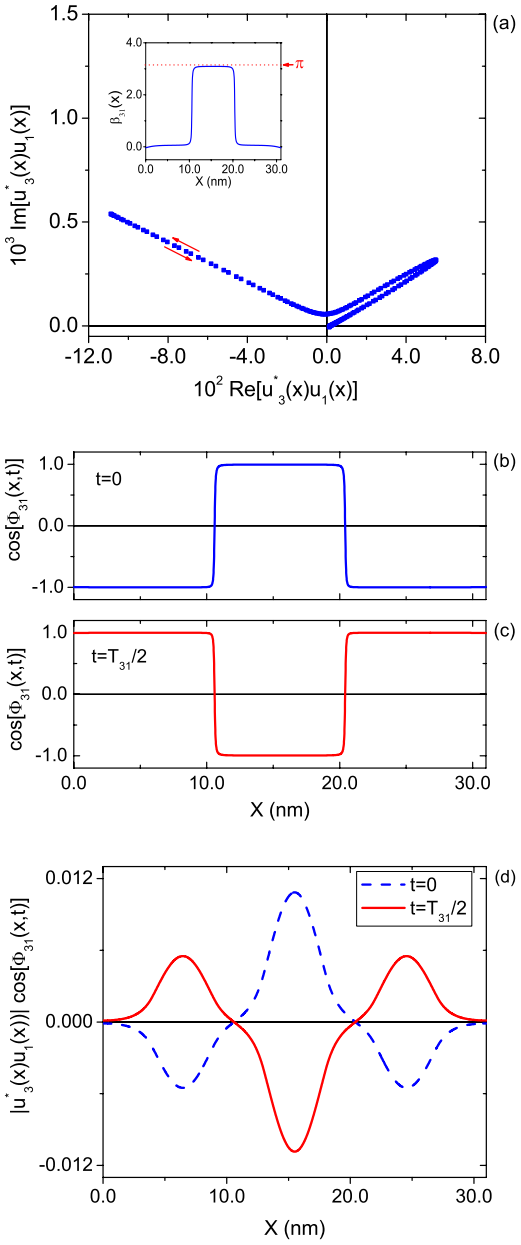

FIG. 5. (Color online) (a) Values of the product $u_3^*(x)u_1(x)$ in the complex plane as x varies from 0 to L. The red arrows indicate that the curve is traced twice as the parameter x varies along the whole interval $[0,L]$. There are dramatic changes in the phase of this quantity that is better appreciated in the inset. The value of the oscillatory function $\Phi_{mn}(x,t)$ in Eq. (11) is evaluated in (b) and (c), respectively, at $t=0$ and $t=T_{31}/2$. The factor $|u_3^*(x)u_1(x)|$ simply modulates this oscillation as illustrated in (d).

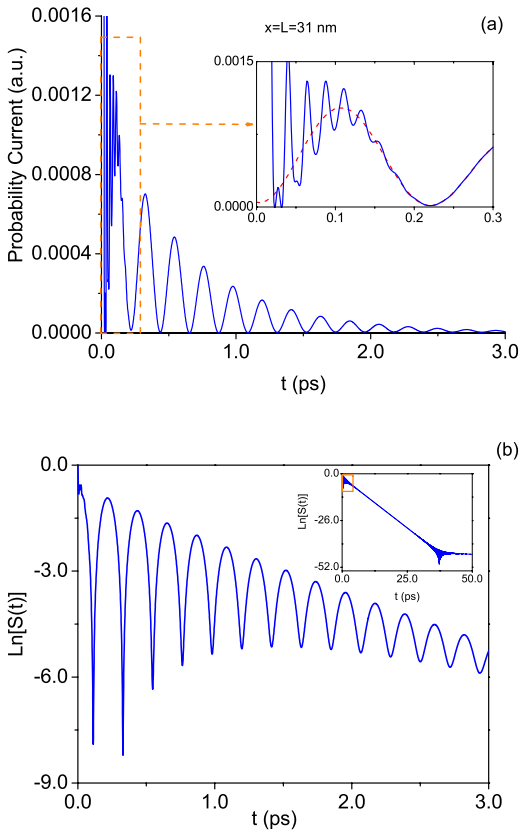

FIG. 6. (Color online) (a) Probability current at the right end of the system, $x=L=31.0$ nm. The outward flux is periodically interrupted each time the initial state is reconstructed in the central well, a process that occurs at the Rabi frequency Ω_{31}. The inset shows Rabi oscillations of higher frequencies due to transitions among far away resonances. Here we compare the calculation with $N=3$ (dashed red line) and $N=9$ (solid blue line). (b) Rabi oscillations of the corresponding survival probability $S(t)$ as a function of time. The inset shows $S(t)$ in a wider time interval that includes the exponential-nonexponential transition at long times. See text.

3. Relationship to the decay process

Figure 6(a) shows the behavior of $J(L,t)$ as a function of time to illustrate the effect of the internal dynamics discussed above on the behavior of the decay process in this transient time domain. The graph exhibits a *pulsed decay* in which the outward flux is periodically interrupted with a frequency that is characteristic of the transitions between the resonance levels of the system. In this case, the oscillatory behavior is also dominated by the Rabi frequency Ω_{31}, and as the inset shows, other Rabi frequencies are also observed at shorter time intervals.

Figure 6(b) exhibits the corresponding oscillatory behavior with time of the survival probability along this regime calculated using Eq. (22). As can be easily verified by inspection of the graphs, the spatial oscillations in Fig. 3 and the oscillatory behavior observed in Fig. 6(b) have exactly the same period, which shows that the oscillatory behavior of the survival probability is linked to the dynamics of the probability density inside the system.

4. Other locations for $\psi(x,0)$: The bouncing mode

The dynamics of the system has a strong dependence on the location of the initial state. A variation in the spatial location of $\psi(x,0)$ may affect dramatically the dynamics of both the internal probability density and the pulsed decay. If, for example, the initial pulse is placed off the center of the system (say, at the left lateral well) the selection rule mentioned above no longer applies and transitions between resonant states with both n odd and even will be allowed. The

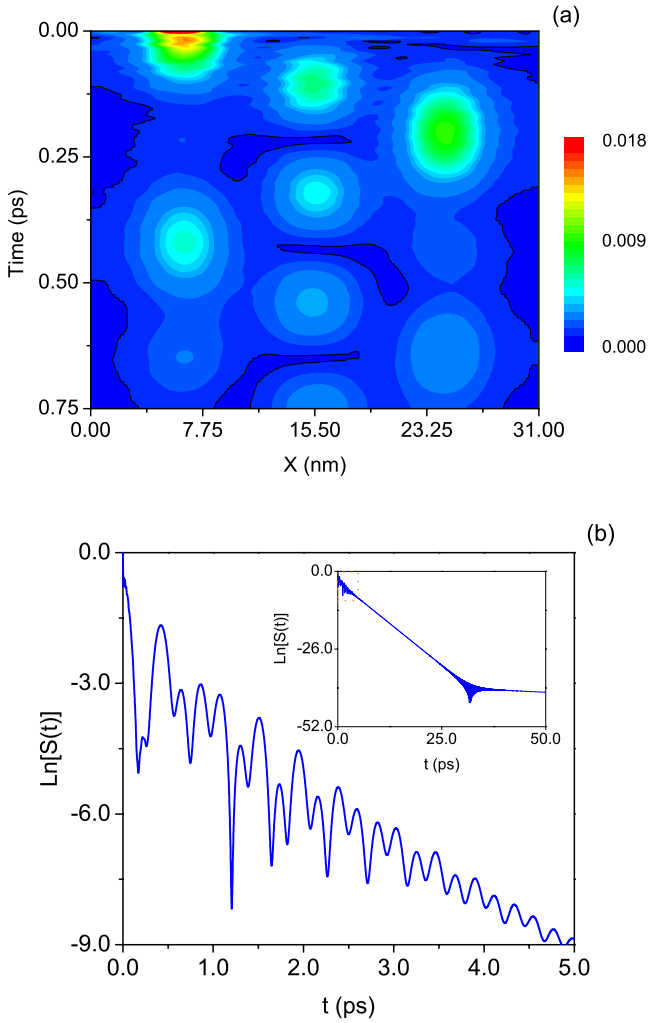

FIG. 7. (Color online) (a) Dynamics of the probability density $|\psi(x,t)|^2$ showing a "bouncing" behavior along the same periodic quadruple barrier system of the previous figures but with the initial state located in the first (left) well. (b) Rabi oscillations of the corresponding survival probability $S(t)$ as a function of time exhibiting a more complex behavior. The inset shows $S(t)$ in a wider time interval that includes the exponential-nonexponential transition at long times. See text.

regularities in the dynamics of $|\psi(x,t)|^2$ remain now in the form of a *bouncing* motion of the maximum of the probability density in the X-t plane that has some resemblance with the classical picture of a particle bouncing inside the system, as displayed in Fig. 7(a). The mixture of the various Rabi frequencies yields a more complex behavior of the survival probability, as depicted in Fig. 7(b).

IV. CONCLUDING REMARKS

The process of quantum decay in multibarrier resonance structures was analyzed using an exact analytical approach. The mechanism of pulsed quantum decay is shown to be directly related to a cyclic process of the maximum value of the probability density inside the system, which consists of spatial oscillations of the probability density that arise from resonance state interference. This is a result worth stressing out since we are accounting for an internal oscillatory process that governs the dynamics of decay and provides a specific imprint of that behavior on the time evolution of the survival probability.

It is worth mentioning the relevant role played in the present work by Eq. (8), which provides a representation for the time evolution of the decaying wave function as a discrete expansion in terms of the resonance states of the problem, and by Eq. (7), which establishes a condition for the corresponding expansion coefficients that allows to keep a finite number of terms in the resonance expansion. We have shown that resonance states may be handled in a fashion very similar to bound states to describe the complex internal dynamics of decay in multibarrier systems.

Recently it came to our notice a work that discusses the decay of an initial state formed by wave packet scattering on a multibarrier system [17,18]. A distinctive feature of this approach is that the initial state is quasistationary, its formation involving a finite buildup time. In order to describe a decay process, in this approach the quasistationary state must possess a lifetime large enough to avoid interference with the transmitted and reflected scattering wave packets. The initial quasistationary state results from a complex transient behavior involving the whole system. This implies, strictly, that the initial quasistationary state extends beyond the limits of the system and hence it differs from the initial states, which are localized in a given well, as considered in our work. As a consequence they do not address the calculation of the survival probability. The examples discussed by the authors of Ref. [18] exhibit some beats in the probability density and the probability current density calculated, respectively, along the external region and the edge points of the multibarrier system. Apparently, these beats have some resemblance with the bouncing mode discussed in our work. It is not evident that the scattering approach may lead to the formation of a quasistationary state confined initially to a small region of the system and hence capable of producing the breathing and bouncing modes that we have discussed. Certainly, it would be of interest to make a comparison of that approach with ours. It is worth mentioning here that the case of scattering by an infinitely broad wave packet, i.e., a plane wave, in a quantum shutter setup has been solved analytically in Ref. [19].

We end our discussion by pointing out that regarding experiment it is necessary to extend to multibarrier systems the techniques used to verify the exponential decay law in double-barrier resonant structures [20]. However, it might be that to test the oscillatory decaying behavior discussed here may require of a new type of experimental setup. Regarding the dynamics of the probability density along the internal region of the multibarrier structure, an interesting possibility is to create the initial wave packet by an ultrafast laser source and make use of specific spectroscopies to observe the oscillatory motion of the wave packet [11]. Our results are of a general validity in quantum mechanics and hence one may consider other artificial multibarrier structures as ultracold atomic gases in optical lattices [21] and in optical tests of quantum mechanics [22].

[1] G. Gamow, Z. Phys. **51**, 204 (1928).
[2] R. W. Gurney and E. U. Condon, Phys. Rev. **33**, 127 (1929).
[3] L. A. Khalfin, Sov. Phys. Dokl. **2**, 340 (1957); Sov. Phys. JETP **6**, 1053 (1958).
[4] S. R. Wilkinson, C. F. Bharucha, M. C. Fischer, K. W. Madison, P. K. Morrow, Q. Niu, B. Sundaram, and M. G. Raizen, Nature (London) **387**, 575 (1997).
[5] C. Rothe, S. I. Hintschich, and A. P. Monkman, Phys. Rev. Lett. **96**, 163601 (2006).
[6] R. G. Winter, Phys. Rev. **123**, 1503 (1961).
[7] T. Jittoh, S. Matsumoto, J. Sato, Y. Sato, and K. Takeda, Phys. Rev. A **71**, 012109 (2005).
[8] P. Exner and M. Fraas, J. Phys. A **40**, 1333 (2007).
[9] G. García-Calderón, I. Maldonado, and J. Villavicencio, Phys. Rev. A **76**, 012103 (2007).
[10] D. K. Ferry and S. M. Goodnick, *Transport in Nanostructures* (Cambridge University Press, United Kingdom, 1997).
[11] K. Leo, J. Shah, E. O. Göbel, T. C. Damen, S. Schmitt-Rink, W. Schäfer, and K. Köhler, Phys. Rev. Lett. **66**, 201 (1991).
[12] A. Chomette, B. Deveaud, A. Regreny, and G. Bastard, Phys. Rev. Lett. **57**, 1464 (1986).
[13] G. García-Calderón, R. Romo, and J. Villavicencio, Phys. Rev. B **76**, 035340 (2007).
[14] G. García-Calderón, J. L. Mateos, and M. Moshinsky, Phys. Rev. Lett. **74**, 337 (1995).
[15] See Appendix A in G. Garcia-Calderon and A. Rubio, Phys. Rev. A **55**, 3361 (1997).
[16] G. García-Calderón and J. Villavicencio, Phys. Rev. A **73**, 062115 (2006).
[17] Yu. G. Peisakhovich and A. A. Shtygashev, Phys. Rev. B **77**, 075326 (2008).
[18] Yu. G. Peisakhovich and A. A. Shtygashev, Phys. Rev. B **77**, 075327 (2008).
[19] G. Garcia-Calderon and A. Rubio, Phys. Rev. A **55**, 3361 (1997); R. Romo and J. Villavicencio, Appl. Phys. Lett. **78**, 1769 (2001).
[20] M. Tsuchiya, T. Matsusue, and H. Sakaki, Phys. Rev. Lett. **59**, 2356 (1987).
[21] M. Lewenstein, A. Sanpera, V. Ahufinger, D. Bogdan, A. Sen, and U. Sen, Adv. Phys. **56**, 243 (2007).
[22] S. Longhi, Phys. Rev. Lett. **97**, 110402 (2006).